Archives of Control Sciences, 2003, **13**, (2), pp. 117–139.

Adaptive Active Control of Noise and Vibration

M. O. TOKHI

This paper presents the development of a unified approach to active control of noise and vibration. The design of an active control system is initially considered on the basis of a single-input single-output (SISO) structure. The design procedure is formulated so as to allow on-line adaptation and control, and accordingly an adaptive control algorithm is devised. The design is then extended to the case of a single-input multi-output (SIMO) control structure. The control strategies thus devised are verified in the cancellation of broadband noise in a free-field medium, and in vibration suppression in a cantilever beam in fixed-free and fixed-fixed modes. A comparative assessment of the results with SISO and SIMO control structures is presented and discussed.

Keywords: Active noise control, active vibration control, adaptive control, self-tuning control.

1. Introduction

Noise and vibration have long been recognised as sources of environmental pollution, having adverse effects on human life in numerous ways. Many attempts have been made in the past at devising methods of tackling the problems arising from unwanted noise and vibration. Traditional methods of noise cancellation and vibration suppression utilise passive control techniques, which consist of mounting layers of passive material on or around the source. Investigations have shown that these methods are efficient at high frequencies but expensive and bulky at low frequencies [1].

Active control of noise/vibration consists of artificially generating cancelling source(s) to destructively interfere with the unwanted source and thus result in a reduction in the level of the noise/vibration at desired location(s). Active noise/vibration control (active control) is not a new concept. It is based on the principles that were initially proposed by Lueg in the early 1930s for noise cancellation [2]. Since then a considerable amount of research work has been devoted to the development of methodologies for the design and realisation of active control systems in various applications [1], [3], [4], [5], [6].

In many practical applications the problem of noise and vibration are closely related. For example, a close coherence is observed in numerous situations between the two due to secondary effects. Many sources of noise, for instance, vibrate and the vibration is found to be coherent with the acoustic waves they emit. It is often noticed in buildings, for instance, that noise due to chattering of windows or motion of articles is caused through ground vibrations by passing trains and/or vehicles. In these cases a control solution aimed at reducing, for example, the level of vibration will result in significant reduction in the level of noise and, to some extent, vice versa. Moreover, the control of noise and vibration by active means is based on the same design principle. These form the basis of design unification in this work by adopting a systems approach for the development of an active control strategy for both noise cancellation and vibration suppression. Thus, the method presented here can be utilised to tackle the problem of noise and vibration either in isolation or together. The results presented in this paper, however, correspond to the former.

Due to the broadband nature of noise/vibration (disturbances), it is required that active controllers realise suitable frequency-response characteristics so that cancellation over a broad range of frequencies is achieved [1], [7]. Moreover, due to the time-varying nature of disturbances and characteristics of system components the control mechanism is further required

---

The author is with the Department of Automatic Control and Systems Engineering, The University of Sheffield, UK.
Email: o.tokhi@sheffield.ac.uk

to be intelligent enough to track such variations, so that the desired level of performance is achieved and maintained.

Through his experiments of reducing transformer noise, Conover was the first to realise the need for a 'black box' controller that would adjust the cancelling signal in accordance with information gathered at a remote distance from the transformer [8]. Later it has been realised by numerous researchers that an essential requirement for an active noise/vibration control system to be practically successful is to have an adaptive capability [1], [9], [10], [11], [12], [13]. Implementing an adaptive control algorithm within an active control system will allow the controller characteristics to be adjusted in accordance with changes in the system.

Chaplin and his associates reported some success with an adaptive scheme based on a trial and error waveform generation [10], [14], [15]. Their method relied on the source noise being periodic. The method has been tested with rotary machines such as motor vehicle, fan, etc. where the noise spectrum is harmonically related to the fundamental (engine firing) frequency. The engine firing frequency provides a clock signal to the algorithm. Noticeable amounts of theoretical and practical work have subsequently been reported in the area of adaptive active control [11], [15], [16], [17], [18], [19], [20], [21], [22], [23], [24], [25], [26], [27]. Among these the scheme developed by Eriksson and his co-workers relies on the development of a model of the source. The scheme reported by Nelson, Elliott and co-workers is based on minimisation (in the least square sense) of sound level at discrete locations in the medium. The control scheme reported by Tokhi and Leitch is based on optimum cancellation of disturbances. The work presented here extends the latter to incorporate multiple cancelling sources.

Active control mechanisms developed generally concentrate on reducing the level of the disturbances at selective frequencies or at narrow bands. In doing so, problems related to observation and/or control spill-over due to un-modelled dynamics of the system arise. These problems can be avoided by designing an active control system that incorporates a suitable system identification algorithm through which an appropriate model of the system can be developed within a broad frequency range of interest. The active control system development presented in this paper includes an on-line system identification algorithm, which gives a suitable model of the system in parametric form within a broad range of frequencies of interest. The model thus obtained is then used to design the required controller and generate the corresponding control signal so that to reduce the level of the disturbance over this broad frequency range.

The superposition of the component waves in an active control system results in an interference pattern throughout the medium in which the level of cancellation in some regions will be higher and in some regions it will be lower or even will correspond to reinforcement. The level and physical extent of cancellation achieved is primarily dependent on the geometrical arrangement of system components. Moreover, the number of secondary sources, depending on limitations due to physical dimensions, has a significant effect on the level as well as physical extent of cancellation [28].

This paper considers the development of active adaptive control systems for noise cancellation and vibration suppression. The paper is structures as follows: Section 2 presents the design of an active control system on the basis of a single-input single-output (SISO) structure. The design procedure is formulated so as to allow on-line adaptation and control, and accordingly an adaptive control algorithm is devised. The design is then extended to the case of a single-input multi-output (SIMO) control structure. The control strategies thus devised are verified in the cancellation of broadband noise in a free-field medium. A flexible beam system in transverse vibration is considered for vibration suppression in Section 3. The self-tuning control algorithm developed within the ANC system is used and implemented within SISO and SIMO active vibration control (AVC) structures and its performance assessed in the vibration suppression of the flexible beam system in fixed-free and fixed-fixed modes. The paper is concluded in Section 4.

2. Active noise control

A schematic diagram of the geometric arrangement of a SIMO ANC structure is shown in Figure 1(a). The (unwanted) primary noise is detected by a detector (sensor), located at a distance r_e relative to the primary source and distance r_{fi} relative to secondary (cancelling) source i ($i = 1,\ldots,k$). The detected signal is processed by a SIMO controller of suitable frequency-dependent characteristics and fed to a set of k secondary sources. The secondary signals thus generated interfere with the primary noise so that to achieve a reduction in the level of the noise at and in the vicinity of observation points j ($j = 1,\ldots,k$), located at distances r_{gj} relative to the primary source and r_{hij} relative to secondary source i, in the medium.

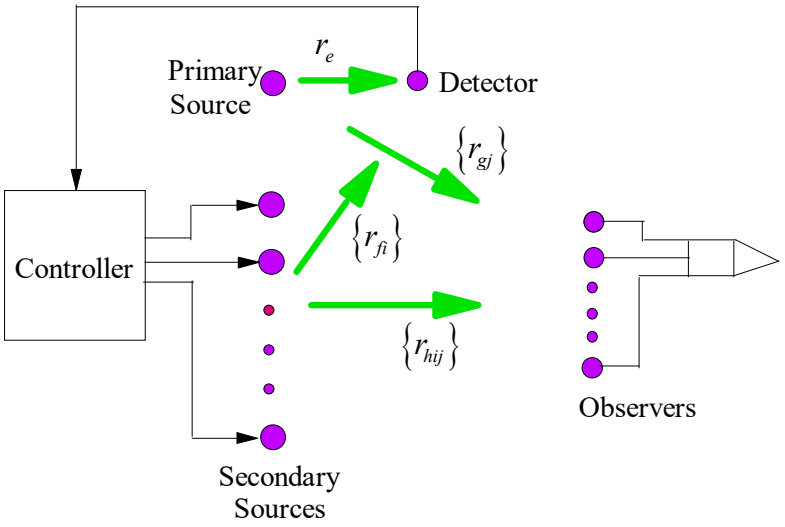

(a) Schematic diagram.

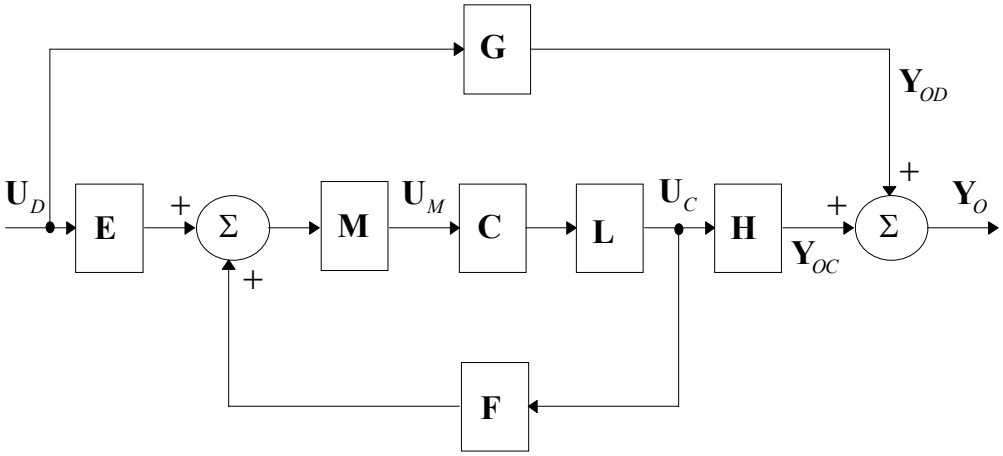

(b) Block diagram.

Figure 1. Active noise control structure.

A frequency-domain equivalent block diagram of the ANC structure is shown in Figure 1(b), where, $\mathbf{E} = [e]$ is a 1×1 matrix representing the transfer characteristics of the path, through the distance r_e, between the primary source and the detector, $\mathbf{F}$ is a $k \times 1$ matrix representing the transfer characteristics of the paths, through the distances r_{fi} ($i = 1,\ldots,k$), from the secondary sources to the detection point, $\mathbf{G}$ is a $1 \times k$ matrix representing the transfer characteristics of the

paths, through the distances r_{gj} ($j = 1,\ldots,k$), from the primary source to the observation points, $\mathbf{H}$ is a $k \times k$ matrix representing the transfer characteristics of the paths, through the distances r_{hij}, from the secondary sources to the observation points, $\mathbf{M} = [m]$ is a 1×1 matrix representing the transfer characteristics of the detector, $\mathbf{L}$ is a $k \times k$ diagonal matrix representing the transfer characteristics of the secondary sources and $\mathbf{C}$ is a $1 \times k$ matrix representing the transfer characteristics of the controller;

$$\mathbf{F} = [f_1 \quad f_2 \quad \cdots \quad f_k]^T, \quad \mathbf{G} = [g_1 \quad g_2 \quad \cdots \quad g_k], \quad \mathbf{C} = [c_1 \quad c_2 \quad \cdots \quad c_k],$$
$$\mathbf{H} = \begin{bmatrix} h_{11} & h_{12} & \cdots & h_{1k} \\ h_{21} & h_{22} & \cdots & h_{2k} \\ \vdots & \vdots & \vdots & \vdots \\ h_{k1} & h_{k2} & \cdots & h_{kk} \end{bmatrix}, \quad \mathbf{L} = \begin{bmatrix} l_1 & 0 & \cdots & 0 \\ 0 & l_2 & \cdots & 0 \\ \vdots & \vdots & \vdots & \vdots \\ 0 & 0 & \cdots & l_k \end{bmatrix} \tag{1}$$

$\mathbf{U}_D$ is a 1×1 matrix representing the disturbance (primary) signal at the source, $\mathbf{Y}_{OD}$ is a $1 \times k$ matrix representing the primary signal at the observation points, $\mathbf{U}_C$ is a $1 \times k$ matrix representing the control (secondary) signals at the source, $\mathbf{Y}_{OC}$ is a $1 \times k$ matrix representing the control signals at the observation points, $\mathbf{U}_M$ is a 1×1 matrix representing the detected signal and $\mathbf{Y}_O$ is a $1 \times k$ matrix representing the observed signals.

The block diagram in Figure 1(b) can be thought either in the continuous complex frequency, s, domain or in the discrete complex frequency, z, domain. The analysis and design presented in this paper apply equally to both domains. The implementation of the controller, however, is carried out in the discrete-time domain.

The control structure in Figure 1 corresponds to the basic structure proposed by Lueg in his patent where the time delay is implemented by the physical separation between the primary and secondary sources [1]. A significant amount of consideration has subsequently been given to this structure in various applications. Conover, Hesselmann and Ross have employed this structure in the cancellation of transformer noise [8], [29], [30]. Ross has considered the design, Roure has analysed the stability, Eriksson, et al. have considered the implementation of this structure in the cancellation of the one-dimensional duct noise [13], [18], [19], [21], [31]. Nelson, et al. have analysed the performance of this structure in the cancellation of enclosed sound fields [32], [33], [34]. Tokhi and Leitch have considered the design, stability, performance and implementation of this structure in the cancellation of noise in three-dimensional propagation [1], [7], [25], [26], [35], [36].

The objective in Figure 1 is to achieve full (optimum) cancellation at the observation points. This is equivalent to the minimum variance design criterion in a stochastic environment. This requires the primary and secondary signals at each observation point to be equal in amplitudes and have a phase difference of 180^0 relative to one another;

$$\mathbf{Y}_O = \mathbf{Y}_{OD} + \mathbf{Y}_{OC} = 0 \tag{2}$$

Using the block diagram in Figure 1(b) the signals $\mathbf{Y}_{OD}$ and $\mathbf{Y}_{OC}$ can be obtained as

$$\begin{aligned} \mathbf{Y}_{OD} &= \mathbf{U}_D\mathbf{G} \\ \mathbf{Y}_{OC} &= \mathbf{U}_D\mathbf{EGMCL}[\mathbf{I} - \mathbf{FMCL}]^{-1}\mathbf{H} \end{aligned} \tag{3}$$

where $\mathbf{I}$ is the identity matrix. Substituting for $\mathbf{Y}_{OD}$ and $\mathbf{Y}_{OC}$ from equation (3) into equation (2) and solving for $\mathbf{C}$ yields

$$\mathbf{C} = \mathbf{M}^{-1}\left[\mathbf{G}\mathbf{H}^{-1}\mathbf{F} - \mathbf{E}\right]^{-1}\mathbf{G}\mathbf{H}^{-1}\mathbf{L}^{-1} \tag{4}$$

This is the required controller transfer function for optimum cancellation of broadband noise at the observation points. The controller thus designed is assured to be causal by making the number of zeros in each path either equal to or less than the number of poles accordingly. Note that, for given secondary sources and detection sensor the characteristics of the required controller are determined by the geometric arrangement of system components. Among these, it is possible with some arrangements that the determinant $\left|\mathbf{G}\mathbf{H}^{-1}\mathbf{F} - \mathbf{E}\right|$ will be zero or close to zero, requiring the controller to have impractically large gains. Moreover, with some geometrical arrangements of system components, the (positive) feedback loops due to the secondary signals reaching the detection point can cause the system to become unstable. Therefore, for the system performance to be robust, a consideration of the system in relation to the geometric arrangement of system components is important at a design stage [28], [36], [37].

2.1. Self-tuning active noise control

The design relation given for the controller transfer function in equation (4) is in a form that is not suitable for on-line implementation. To allow on-line design and implementation of the controller, equivalent design rules based on on-line measurement of (input/output) signals of the system are required. To devise such a strategy, a self-tuning-like control mechanism is developed [38], [39], [40].

Consider Figure 1 with measurable input and output signals as the detected signal $\mathbf{U}_M$ and the observed signal $\mathbf{Y}_O$ respectively. Thus, owing to the state of each secondary source, a model of the system between the detection point and each observation point can be obtained. This will result in a set of models with equivalent transfer functions denoted by q_{oj} ($j = 1,\ldots,k$) when all the secondary sources are *off* and a further set of models with equivalent transfer functions denoted by q_{ij} when all the secondary sources are off except secondary source *i*. In this manner, a total of $k(k+1)$ models can be constructed.

Using the block diagram in Figure 1(b), the detected signal $\mathbf{U}_M$ and the observed signal $\mathbf{Y}_O$ can be obtained as

$$\begin{aligned} \mathbf{U}_M &= \mathbf{U}_D\mathbf{E}\mathbf{M}(\mathbf{I} - \mathbf{C}\mathbf{L}\mathbf{F}\mathbf{M})^{-1} \\ \mathbf{Y}_O &= \mathbf{U}_D\left\{\mathbf{G} + \mathbf{E}\mathbf{M}\mathbf{C}\mathbf{L}(\mathbf{I} - \mathbf{F}\mathbf{M}\mathbf{C}\mathbf{L})^{-1}\mathbf{H}\right\} \end{aligned} \tag{5}$$

Thus, the equivalent transfer functions of system's models, for the corresponding situation under consideration, is given by the ratio $\mathbf{Y}_O\mathbf{U}_M^{-1}$ in equation (5).

Substituting for $\mathbf{E}$, $\mathbf{F}$, $\mathbf{G}$, $\mathbf{H}$, $\mathbf{L}$ and $\mathbf{C}$ from equation (1) into equation (4) and simplifying yields a relation for each element of $\mathbf{C}$ as

$$c_i = \frac{1}{b_i}\frac{\sum_{j=1}^{k} g_j H_{ij}}{\sum_{i=1}^{k} f_i\left(\sum_{j=1}^{k} g_j H_{ij}\right) - e|\mathbf{H}|} \tag{6}$$

where, $i = 1, \ldots, k$ and c_i is the ith element of $\mathbf{C}$, $b_i = \mathbf{M}l_i = ml_i$ with l_i representing the transfer characteristics of secondary source i, g_j represents the transfer characteristics of the path, through the distance r_{gj}, between the primary source and observation point j,

$$H_{ij} = (-1)^{i+j} \begin{vmatrix} h_{11} & h_{12} & \cdots & h_{1(j-1)} & h_{1(j+1)} & \cdots & h_{1k} \\ h_{21} & h_{22} & \cdots & h_{2(j-1)} & h_{2(j+1)} & \cdots & h_{2k} \\ \vdots & \vdots & \vdots & \vdots & \vdots & \vdots & \vdots \\ h_{(i-1)1} & h_{(i-1)2} & \cdots & h_{(i-1)(j-1)} & h_{(i-1)(j+1)} & \cdots & h_{(i-1)k} \\ h_{(i+1)1} & h_{(i+1)2} & \cdots & h_{(i+1)(j-1)} & h_{(i+1)(j+1)} & \cdots & h_{(i+1)k} \\ \vdots & \vdots & \vdots & \vdots & \vdots & \cdots & \vdots \\ h_{k1} & h_{k2} & \cdots & h_{k(j-1)} & h_{k(j+1)} & \cdots & h_{kk} \end{vmatrix}$$

with h_{ij} representing the transfer characteristics of the path, through the distance r_{hij}, between secondary source i and observation point j and $|\mathbf{H}|$ represents the determinant of the matrix $\mathbf{H}$.

To obtain c_i in equation (6) in terms of the transfer functions of system models, two cases, namely, when all secondary sources are *off* and when only secondary source i is *on*, are considered (the primary source is *on* throughout).

To switch *off* all secondary sources the 'controller' in Figure 1(a) is replaced with an 'open' switch. This in terms of the block diagram in Figure 1(b) is equivalent to all entries in $\mathbf{C}$ initialised to zero;

$$\mathbf{C} = \mathbf{C}_0 = \begin{bmatrix} 0 & 0 & \cdots & 0 \end{bmatrix} \tag{7}$$

Substituting for $\mathbf{C}$ from equation (7) into equation (5) and simplifying yields the equivalent transfer functions q_{oj} ($j = 1, \ldots, k$) as

$$q_{oj} = \frac{g_i}{me} \; ; \quad j = 1, \ldots, k \tag{8}$$

To keep only secondary source i *on* the 'controller' in Figure 1(a) is replaced by a switch in which only the path through to secondary source i is closed. This in terms of the block diagram in Figure 1(b) is equivalent to the matrix $\mathbf{C}$ initialised to unity at location i and to zero in all other locations;

$$\mathbf{C} = \mathbf{C}_i = \begin{bmatrix} 0 & \cdots & 0 & 1 & 0 & \cdots & 0 \end{bmatrix} \tag{9}$$

Note in equation (9) that, for simplicity purposes, element i of the controller is initialised to unity in this case. Note further that the feedback loop formed through secondary source i to the detector by switching on the corresponding controller path may cause the system to become unstable. Under such a situation the choice of utilising an initial transfer function instead of the switch may be favoured to bring the loop gain below unity and thus allow the system to be stable during the identification phase.

Substituting for $\mathbf{C}$ from equation (9) into equation (5), simplifying and using equation (8) yields

$$\left(\frac{h_{ij}e}{g_j} - f_i\right) b_i = \frac{q_{ij}}{q_{oj}} - 1; \quad i = 1,\ldots,k \text{ and } j = 1,\ldots,k \tag{10}$$

Adding the relations for $i = 1$ to k in equation (10) yields

$$\sum_{i=1}^{k}\left(\frac{h_{ij}e}{g_j} - f_i\right) b_i = \frac{1}{q_{oj}}\sum_{i=1}^{k} q_{ij} - k; \quad j = 1,\ldots,k \tag{11}$$

Equation (11) corresponds to the system description in Figure 1 when all the secondary sources are switched on; i.e. all entries in the matrix **C** initialised to unity. Solving this equation for b_i ($i = 1,\ldots,k$), manipulating each and using equation (6) yields

$$\frac{1}{c_i} = 1 - \frac{1}{W_i}\left\{\sum_{j=1}^{k}\frac{g_j V_{ij}}{q_{oj}}\left(\sum_{p=1}^{k} q_{pj} - k + 1\right)\right\} \tag{12}$$

where, $i = 1, \ldots, k$, and

$$V_{ij} = (-1)^{i+j}\begin{vmatrix} e & f_1 & \cdots & f_{(i-1)} & f_{(i+1)} & \cdots & f_k \\ g_i & h_{11} & \cdots & h_{(i-1)1} & h_{(i+1)1} & \cdots & h_{k1} \\ \vdots & \vdots & \vdots & \vdots & \vdots & \vdots & \vdots \\ g_{j-1} & h_{1(j-1)} & \cdots & h_{(i-1)(j-1)} & h_{(i+1)(j-1)} & \cdots & h_{k(j-1)} \\ g_{j+1} & h_{1(j+1)} & \cdots & h_{(i-1)(j+1)} & h_{(i+1)(j+1)} & \cdots & h_{k(j+1)} \\ \vdots & \vdots & \vdots & \vdots & \vdots & \vdots & \vdots \\ g_k & h_{1k} & \cdots & h_{(i-1)k} & h_{(i+1)k} & \cdots & h_{kk} \end{vmatrix}, \quad W_i = \sum_{j=1}^{k} g_j V_{ij}$$

Simplifying equation (12) and using equations (10) and (11) yields

$$c_i = Q_i\left[\sum_{p=0}^{k} Q_p\right]^{-1}; \quad i = 1,\ldots,k \tag{13}$$

where,

$$Q_o = \begin{vmatrix} q_{11} & q_{12} & \cdots & q_{1k} \\ q_{21} & q_{22} & \cdots & q_{2k} \\ \vdots & \vdots & \vdots & \vdots \\ q_{k1} & q_{k2} & \cdots & q_{kk} \end{vmatrix}, \quad Q_i = (-1)^i \begin{vmatrix} q_{01} & q_{02} & \cdots & q_{0k} \\ q_{11} & q_{12} & \cdots & q_{1k} \\ \vdots & \vdots & \vdots & \vdots \\ q_{(i-1)1} & q_{(i-1)2} & \cdots & q_{(i-1)k} \\ q_{(i+1)1} & q_{(i+1)2} & \cdots & q_{(i+1)k} \\ \vdots & \vdots & \vdots & \vdots \\ q_{k1} & q_{k2} & \cdots & q_{kk} \end{vmatrix}$$

Equation (13) gives the required controller design rules in terms of the transfer characteristics q_{oj} and q_{ij} ($i = 1,\ldots,k$; $j = 1,\ldots,k$) of system models. The controller can thus be designed on-line

by first estimating q_{oj} and q_{ij} using a suitable system identification algorithm, such as the recursive least squares (RLS) algorithm, and then using equation (13) to design the controller. The controller designed in this manner can easily be implemented on a digital processor and the required control signals generated and applied in real-time. Moreover, to achieve on-line adaptation of the controller characteristics whenever a change in the system is sensed, a supervisory level control is required. The supervisor can be designed to monitor system performance and, based on a pre-specified quantitative measure of cancellation, initiate self-tuning control accordingly. In this manner, the actual cancellation achieved at the observation point can be measured, if this is within the pre-specified range then the controller will continue to process the detected signal, generate and output the cancelling signals. If the cancellation, however, is outside the specified limit then self-tuning will be initiated at the identification level. The self-tuning ANC algorithm can be outlined on the basis of the above as follows

(i) Switch off all secondary sources, estimate transfer functions q_{oj} ($j = 1,\ldots,k$).
(ii) Switch on secondary source i ($i = 1,\ldots,k$), estimate transfer functions q_{ij} ($j = 1,\ldots,k$).
(iii) Use equation (13) to obtain the transfer function of the controller c_i ($i = 1,\ldots,k$).
(iv) Implement the controller, to generate the control signals.
(v) Measure system performance and compare with pre-specified index, if within specified range then go to (iv) otherwise go to (i).

Note in the self-tuning ANC algorithm, outlined above, that self-tuning (adaptation) is initiated by the supervisory level control upon detection of degradation in system performance (due to a change in system characteristics). Initiation of self-tuning means that the system transfer characteristics q_{0j} and q_{ij} are re-estimated and the controller re-designed according to equation (13). Although, the self-tuning ANC algorithm preserves the essential features of the traditional self-tuning control by incorporating explicitly the processes of identification and control, thus, the term self-tuning, it does vary from the traditional self-tuning control in that the processes of identification and control are not both executed at each iteration; the process of identification is completed fully in steps (i) and (ii) of the algorithm before commencing the process of control.

It is noted in the self-tuning ANC algorithm above that, to design the controller with k secondary sources, a total of $k(k+1)$ models are required to be identified. This implies that with a large number of secondary sources the computational burden on the processor implementing the algorithm will be significantly high. This will have a corresponding impact on the requirements of the computational capabilities of the processor. Thus, it is important during the process of realisation of the controller, to make sure that the processor meets the on-line sampling requirements of the control scheme as well as provides adequate computing speed for the adaptation mechanism.

In implementing the self-tuning control algorithm described above, several issues of practical importance need to be given careful consideration. These include properties of the disturbance signal, robustness of the estimation and control, system stability and processor-related issues such as word-length, speed and computational power.

In simulation experiments where the primary signal can be chosen properly to satisfy the robustness requirements of the control algorithm problems due to the properties of the input signal will not arise. In practice, however, where the disturbance force may also excite those dynamics of the system, which are not of interest, care must be taken to condition the input signal properly before sampling. Robustness of the control algorithm is related to the accuracy of the estimated plant model. This in turn depends on properties of the input signal, proper initialisation of the parameter estimation algorithm, model order and accuracy of computation [26]. The computational accuracy is related to the processor's dynamic range of computation, determined

by the processor word-length and type of arithmetic. With a processor supporting fixed-point arithmetic for example it is important to take necessary precautions against problems due to overflow and inaccuracies due to truncation/rounding of variables [26].

In employing the minimum variance design criterion, a problem commonly encountered is that of instability of system, specially, when non-minimum phase models are involved. Note in the controller design rules, equation (13), that such a situation will result in a non-minimum phase and unstable controller with the unstable poles approximately cancelling the corresponding zeros that are outside the stability region. Thus, to avoid this problem of instability either the estimated models can be made minimum-phase by reflecting those zeros that are outside the stability region into the stability region and using the resulting minimum-phase models to design the controller or once the controller is designed the poles and zeros that are outside the stability region can be reflected into the stability region. In this manner, a factor $\left(1 - pz^{-1}\right)$ corresponding to a pole/zero at $z = p$, in the complex $z-$plane, that is outside the stability region can be reflected into the stability region by replacing the factor with $\left(p - z^{-1}\right)$.

The supervisory level control described above is used as a performance monitor. In addition to monitoring system performance, it can also be facilitated with further levels of intelligence, for example, monitoring system stability and avoiding problems due to non-minimum phase models as described above, verifying controller characteristics on the basis of practical realisation to make sure that impractically large controller gains are not required as discussed earlier, system behaviour in a transient period, model structure validation etc.

The self-tuning ANC algorithm described above is essentially a model-based adaptive control approach. The controller design rules, satisfying the desired control objectives at optimum cancellation of noise at the observation points, are obtained in terms of characteristics of system models. The development of such design rules allows the formulation of on-line design and implementation of the controller. In this manner, this scheme essentially differs from other adaptive active control schemes, outlined earlier, in two respects: (a) The controller design uses characteristics of system models that are obtained on-line. (b) The design objective is to achieve optimum cancellation (zero disturbance level) at the observation points. In addition to these, in contrast to some of the previously developed methods, which are based on tonal noise cancellation, the proposed scheme looks at broadband cancellation of the noise in an indiscriminate manner, not at selected tones.

2.2. Simulation algorithm

To allow development of a suitable simulation environment for test and verification of the control strategy, consider a loudspeaker, with its drive amplifier, and a microphone incorporating its pre-amplifier, located at a set distance r_m in front of the loudspeaker. This is shown in an equivalent block diagram in Figure 2 where, l represents the transfer characteristics of the loudspeaker, m represents the transfer characteristics of the microphone, $\left(A/r_m\right)exp\left(-j\,r_m\omega/c\right)$ represents the transfer characteristics of the acoustic path through r_m with A as a constant, c as speed of sound and ω the radian frequency. Note that the acoustic medium is assumed to be non-dispersive. Let the amplitude and phase response of the system in Figure 2 from the input of the loudspeaker to the output of the microphone as a function of the frequency ω be denoted by A_m and Q_m respectively;

$$A_m \exp\left(jQ_m\right) = ml\frac{A}{r_m}\exp\left(-j\,r_m\omega/c\right) \tag{14}$$

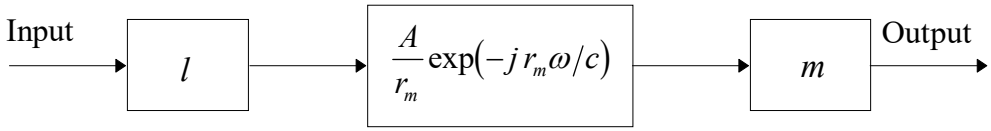

Figure 2. Frequency response measurement.

The frequency response of the acoustic paths through r_e, r_{fi}, r_{gj} and r_{hij} ($i = 1,...,k$; $j = 1,...,k$) in Figure 1 can be written as:

$$\begin{aligned} e(j\omega) &= (A/r_e)\exp(-j\,r_e\omega/c) \\ f_i(j\omega) &= (A/r_{fi})\exp(-j\,r_{fi}\omega/c) \\ g_j(j\omega) &= (A/r_{gj})\exp(-j\,r_{gj}\omega/c) \\ h_{ij}(j\omega) &= (A/r_{hij})\exp(-j\,r_{hij}\omega/c) \end{aligned} \tag{15}$$

Assuming $l_1 = ... = l_k = l$ in equation (1), let $\mathbf{E}'$, $\mathbf{F}'$, $\mathbf{G}'$ and $\mathbf{H}'$ be transfer characteristics defined as

$$\begin{aligned} \mathbf{E}' &= ml\mathbf{E} = \{A_e \exp(jQ_e)\} \\ \mathbf{F}' &= ml\mathbf{F} = \{A_{fi} \exp(jQ_{fi})\} \\ \mathbf{G}' &= ml\mathbf{G} = \{A_{gj} \exp(jQ_{gj})\} \\ \mathbf{H}' &= ml\mathbf{H} = \{A_{hij} \exp(jQ_{hij})\} \end{aligned} \tag{16}$$

Using equations (14), (15) and (16) yields

$$\begin{aligned} A_e &= A_m(r_m/r_e) \quad , \quad Q_e = Q_m - (r_e - r_m)\omega/c \\ A_{fi} &= A_m(r_m/r_{fi}) \quad , \quad Q_{fi} = Q_m - (r_{fi} - r_m)\omega/c \\ A_{gj} &= A_m(r_m/r_{gj}) \quad , \quad Q_{gj} = Q_m - (r_{gj} - r_m)\omega/c \\ A_{hij} &= A_m(r_m/r_{hij}) \quad , \quad Q_{hij} = Q_m - (r_{hij} - r_m)\omega/c \end{aligned} \tag{17}$$

Using equation (16), the controller design relation in equation (4) can equivalently be expressed as

$$\mathbf{C} = \left[\mathbf{G}'\mathbf{H}'^{-1}\mathbf{F}' - \mathbf{E}'\right]^{-1}\mathbf{G}'\mathbf{H}'^{-1}$$

Thus, with given data for A_m and Q_m a suitable simulation environment characterising the system in Figure 1 can be constructed by obtaining the frequency responses $\mathbf{E}'$, $\mathbf{F}'$, $\mathbf{G}'$ and $\mathbf{H}'$ with specified arrangements of the primary source, secondary sources, detector and observers using the corresponding values for r_e, r_{fi}, r_{gj} and r_{hij} and equation (17). This results in an equivalent block diagram of the ANC system as shown in Figure 3. Signal propagation through the system in Figure 1 can thus be simulated using the block diagram in Figure 3 either in the frequency domain or in the time-domain.

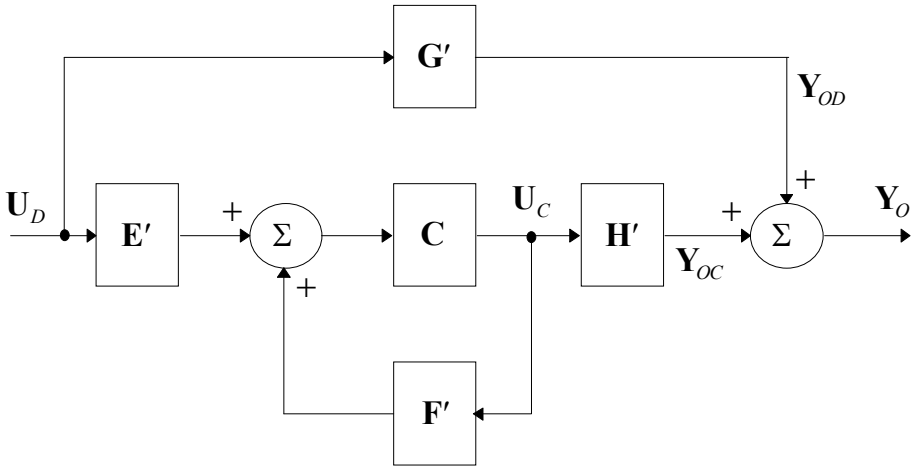

Figure 3. Block diagram of the simulated feedforward ANC structure.

2.3. Implementation and results

To implement the ANC simulation algorithm, an experiment was conducted using the arrangement shown in Figure 2 with $r_m = 0.03$ metres. A sine wave of fixed amplitude and phase was fed into the power amplifier and the frequency varied over the range $0 - 500$ Hz. The amplitude and phase of the microphone output was measured relative to the input and recorded to enable the gain and phase of the system be obtained. The amplitude and phase characteristics of the system thus measured are shown in Figure 4. These were used to realise and implement the simulation environment as outlined above. The algorithm was coded using MATLAB and implemented on a SUN workstation. The self-tuning ANC system was implemented within this environment with a pseudo-random binary sequence (PRBS), simulating a broadband signal in the range $0 - 512$ Hz as the primary noise source. The dynamic range of the simulation environment was extended by interpolating the corresponding measured data so that to match the frequency ranges of the primary signal.

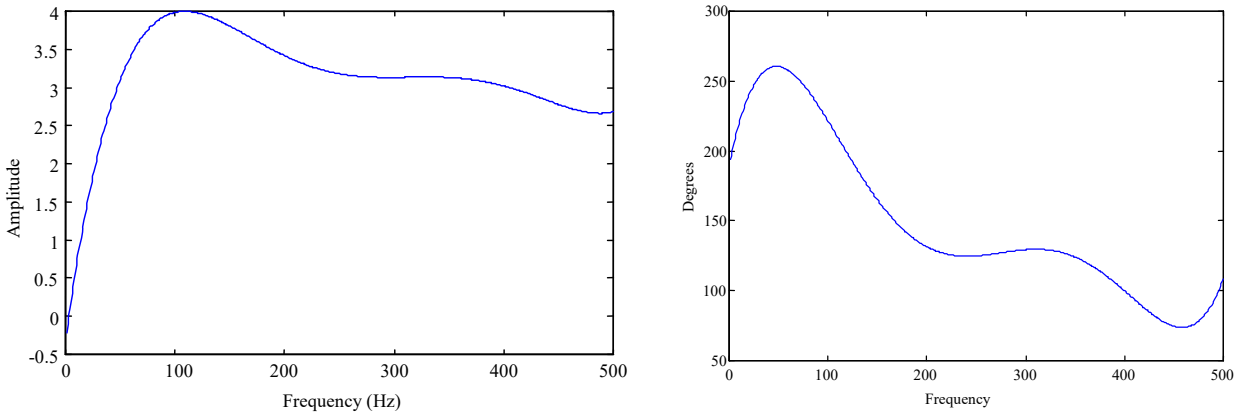

(a) System gain (b) System phase.

Figure 4. Transfer characteristics of loudspeaker-microphone combination.

The system was first realised within a SISO structure with second order models for q_{01} and q_{11}. The auto-power spectral density of the noise was obtained at the observation point before

and after cancellation and their difference giving the cancelled spectrum was evaluated. The performance of the system thus obtained is shown in Figure 5. As noted, an average cancellation level of about 20 dB was achieved over the broad frequency range of 0-512 Hz. Note that the cancellation at frequencies below 25 Hz is lower and decreases with frequency, resulting reinforcement below 20 Hz. This, as noted in Figure 4, is due to the corresponding large signal attenuation occurring in the loudspeaker within this frequency region.

To investigate the performance of the self-tuning active control algorithm with multiple secondary sources, the system was realised within a SIMO structure incorporating two secondary sources and its performance monitored at the observation points. Figure 6 shows the performance of the system under this situation. As noted, an average cancellation level of above 20 dB was achieved at each observation point over the broad frequency range of the noise. A similar trend in the level of cancellation for frequencies below 25 Hz is seen as noted with the SISO system due to the loudspeaker characteristics.

It is noted in Figures 5 and 6 that the self-tuning active control algorithm has performed to a significant level in the cancellation of broadband noise using second order system models. It is possible to enhance the performance of the system further by increasing the orders of the system models. The consequences of this would be an increase in the number of parameters to be identified at the identification stage and an increase in the total execution time of the algorithm, affecting the real-time requirements of the system. However, these problems can be overcome by employing more powerful computing platforms.

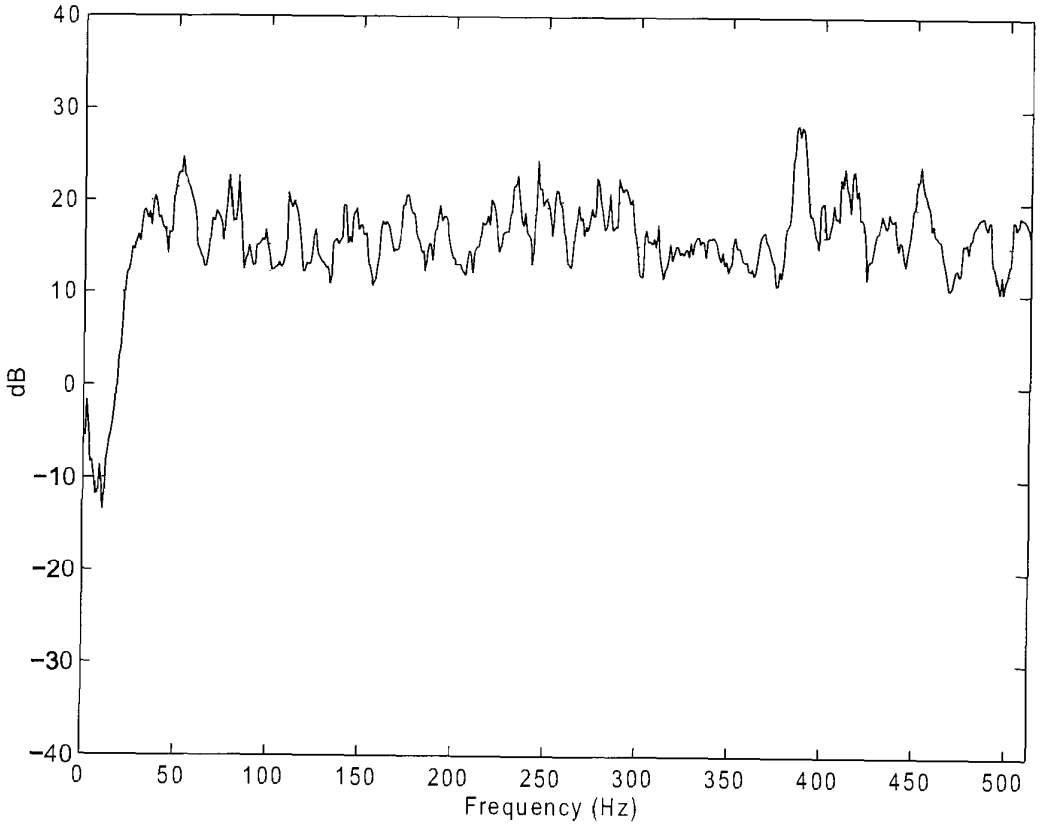

Figure 5. Cancelled spectrum at the observation point with the SISO self-tuning ANC system.

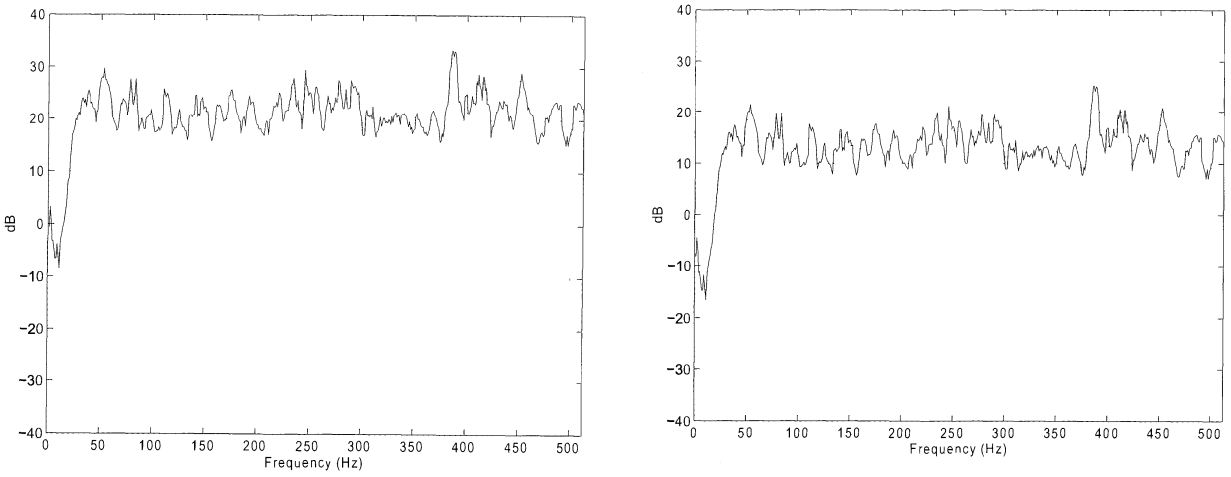

(a) Observation point 1.

(b) Observation point 2.

Figure 6. Cancelled spectrum with the SIMO self-tuning ANC system.

3. Active vibration control

The design of an AVC system depends upon the complexity of the structure under consideration and the nature of the disturbance process. A flexible beam system in transverse vibration is considered here. Such a system has an infinite number of modes although in most cases the lower modes are the dominant ones requiring attention.

A schematic diagram of the AVC system is shown in Figure 7. The unwanted vibrations in the structure are assumed to be due to a single (primary) point disturbance force of broadband nature. These are detected by a point detector, processed by a controller to generate suitable (secondary) suppression signals via point actuator(s) so that to yield vibration suppression over a broad frequency range at observation point(s) along the beam. A frequency-domain equivalent block diagram of the AVC system in Figure 7 will give rise to that of the ANC system in Figure 1(b), with a similar interpretation of the transfer functions and signals involved. In this manner, the required controller transfer function for optimum vibration suppression at the observation points is, therefore, given as in equation (2) with the corresponding equivalent relation suitable for on-line design and implementation as in equation (13). Therefore, a similar formulation of the self-tuning control algorithm developed for noise cancellation applies to vibration suppression in Figure 7, yielding a self-tuning AVC algorithm. To meet the observability and controllability requirements, the system components in Figure 7 are suitably placed relative to one another. For the disturbance signal to be measured properly, for instance, the detector is required to be placed close to the primary source and such that to detect the dynamic modes of interest of the system. Moreover, to achieve vibration suppression over a broad range of frequencies, the actuator should be located such that to excite all the dynamic modes of interest of the beam. Integral to these requirements is, additionally, to ensure that the arrangement results in a practically realisable controller and stable system, as discussed earlier within ANC.

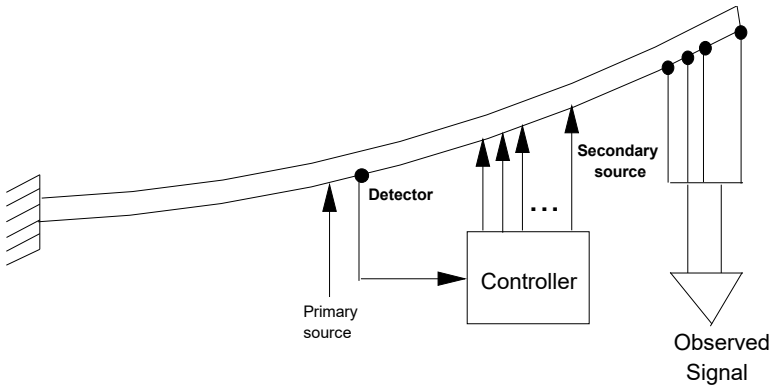

Figure 7. Active vibration control structure.

3.1. Simulation algorithm

Consider a cantilever beam of length L, fixed at one end and free at another, with a force $U(x,t)$ applied at a distance x from its fixed (clamped) end at time t, resulting a deflection $y(x,t)$ of the beam from its stationary (unmoved) position at the point where the force has been applied. The motion of the beam in transverse vibration is, thus, governed by the well-known fourth-order partial differential equation (PDE) [41]

$$\mu^2 \frac{\partial^4 y(x,t)}{\partial x^4} + \frac{\partial^2 y(x,t)}{\partial t^2} = \frac{1}{m} U(x,t) \tag{18}$$

where μ is a beam constant given by $\mu^2 = EI/\rho A$, with ρ, A, I and E representing mass density, cross-sectional area, moment of inertia of the beam and the Young modulus respectively, and m is the mass of the beam. The corresponding boundary conditions at the fixed and free ends of the beam are given by

$$\begin{aligned} y(0,t) = 0 \quad &\text{and} \quad \frac{\partial y(0,t)}{\partial x} = 0 \\ \frac{\partial^2 y(L,t)}{\partial x^2} = 0 \quad &\text{and} \quad \frac{\partial^3 y(L,t)}{\partial x^3} = 0 \end{aligned} \tag{19}$$

Note that the model thus utilised incorporates no damping. To construct a suitable platform for test and verification of the control mechanism, a method of obtaining numerical solution of the PDE in equation (18) is required. This can be achieved by using the finite difference (FD) method. This involves a discretisation of the beam into a finite number of equal-length sections (segments), each of length Δx, and considering the beam motion (deflection) for the end of each section at equally-spaced time steps of duration Δt. Thus, using first-order central FD methods to approximate the partial derivative terms in equations (18) and (19) yields [42], [43]

$$Y_{j+1} = -Y_{j-1} - \lambda^2 S Y_j + (\Delta t)^2 U(x,t) \frac{1}{m} \tag{20}$$

where, Y_k $(k = j-1,\ j,\ j+1)$ is an $n \times 1$ matrix representing the deflection of grid-points 1 to n of the beam at time step k, S is a stiffness matrix, given in terms of characteristics of the beam

and the discretisation steps Δt and Δx, and $\lambda^2 = (\Delta t)^2 (\Delta x)^{-4} \mu^2$. Equation (20) is the required relation for the simulation algorithm, characterising the behaviour of the cantilever beam system, which can be implemented on a digital computer easily. For the algorithm to be stable it is required that the iterative scheme described in equation (20), for each grid point, converges to a solution. It has been shown that a necessary and sufficient condition for stability satisfying this convergence requirement is given by $0 < \lambda^2 \leq 0.25$.

Considering the beam in fixed-fixed form, the corresponding boundary conditions are given by

$$\begin{aligned} y(0,t) &= 0 \quad \text{and} \quad \frac{\partial y(0,t)}{\partial x} = 0 \\ y(L,t) &= 0 \quad \text{and} \quad \frac{\partial y(L,t)}{\partial x} = 0 \end{aligned} \tag{21}$$

Thus, discretisation of the PDE with the boundary conditions for this case can be carried out in a similar manner as for the fixed-free beam. This will result in the same relation given in equation (20) with a new stiffness matrix *S* based on the boundary conditions.

3.2. Implementation and results

In these simulation studies an aluminium type cantilever beam of length $l = 0.635$ m, $m = 0.03745$ kg and $\mu = 1.3511$ is considered. Investigations were carried out to determine a suitable number of segments the beam be divided into so that an adequate level of accuracy is achieved by the simulation algorithm in representing the characteristic behaviour of the beam.

To investigate the performance of the self-tuning AVC algorithm in broadband vibration suppression the beam simulation algorithm for fixed-free form, as a test and evaluation platform, was implemented using 20 grid-points along the beam. The self-tuning algorithm was first realised within a SISO control structure with the primary and secondary sources located at grid points 15 and 19 respectively, the detector at grid-point 15 and the observer at grid-point 11 along the beam. The self-tuning AVC algorithm was implemented on a special-purpose DSP processor and its performance was assessed with a step disturbance force as the unwanted primary disturbance. Figure 8 shows the performance of the system as measured at the observation point, as the difference between the spectra before and after cancellation, i.e. the actual attenuation. The sharp dips noted in Figure 8, correspond to the resonance modes of vibration of the beam. Due to the sudden change of the energy level at the resonance modes (which is more due to use of controller as compared to without controller), the changes at next frequency points are not smooth. Thus, this effect causes more cancellation at the end of the resonance modes.

To investigate the performance of the self-tuning AVC algorithm within a SIMO control structure, a system with two secondary sources located at grid points 17 and 19, was realised. With the primary source and the detector both located at grid point 15, the self-tuning AVC system was implemented to achieve optimum cancellation at grid points 11 (observation point 1) and 9 (observation point 2). Figure 9 shows the corresponding attenuation at the two observation points. It is seen that an average level of cancellation, over the broad frequency range of the disturbance, of at least 40 dB is achieved at each observation point. The sharp dips, noted earlier using the SISO controller as well, occur at the resonance frequencies of vibration of the beam. As compared with the performance of the system using the SISO controller in Figure 8, the amount of cancellation achieved at the lower resonance modes is significantly larger using the SIMO controller. A time-domain description of the performance of the system revealed that the level of

vibration is reduced by 95% throughout the beam length. This demonstrates the capability of the self-tuning AVC algorithm in the suppression of vibration in flexible cantilever beam structures.

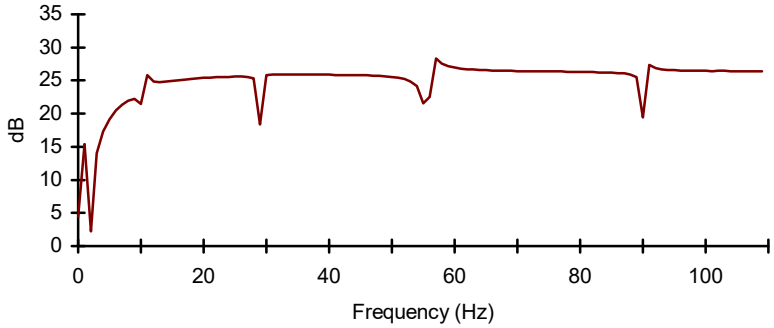

Figure 8. Performance (attenuation in spectral density) of the SISO self-tuning AVC system at observation point.

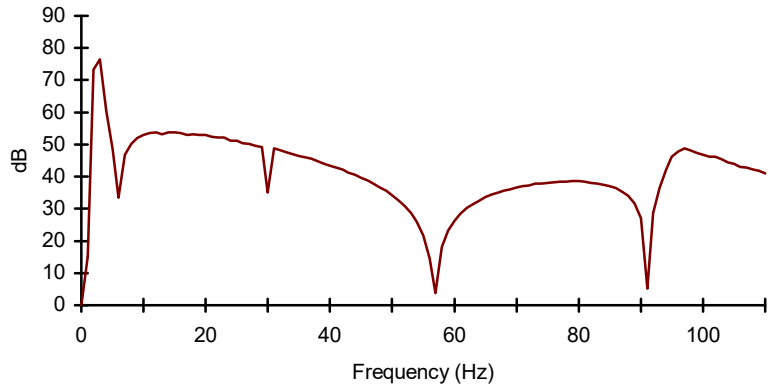

(a) At observation point 1.

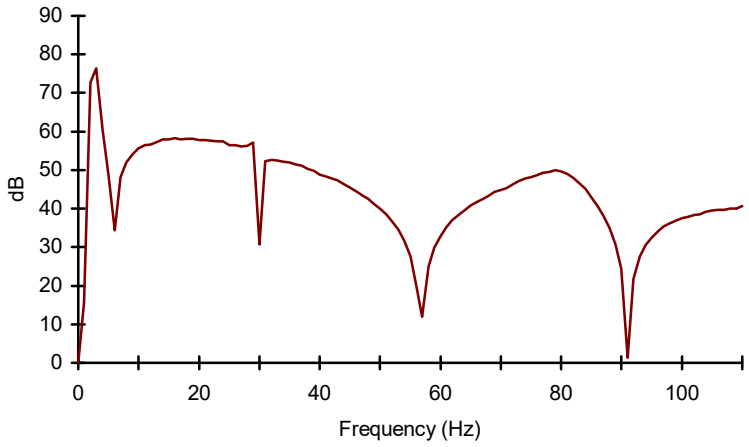

(b) At observation point 2.

Figure 9. Attenuation in spectral density of the disturbance with the SIMO self-tuning AVC system.

A comparison of the performance of the system with the SIMO and SISO controllers is shown in Figure 10 in terms of the average signal power along the beam length before and after cancellation. It is clear from these diagrams that the performance of the system with the SIMO controller is significantly better than that with the SISO controller. This implies that the utilisation of a multiple set of cancelling sources enhances the performance of the system. However, it must be noted that the geometrical arrangement of system components as discussed earlier plays an important role in the performance of the system.

Similar experiments were conducted with the fixed-fixed beam. To demonstrate the capabilities of SISO and SIMO structure, average cancellation of vibration throughout the grid points is shown in Figure 11. A comparison of the performance of the system with the SIMO and SISO controllers reveals that the performance of the system with the SIMO controller is significantly better than that with the SISO controller. This implies that the utilisation of a multiple set of cancelling sources enhances the performance of the system and to a similar level as demonstrated with the fixed-free beam. However, it must be noted again in this case that the geometrical arrangement of system components as discussed earlier plays an important role in the performance of the system.

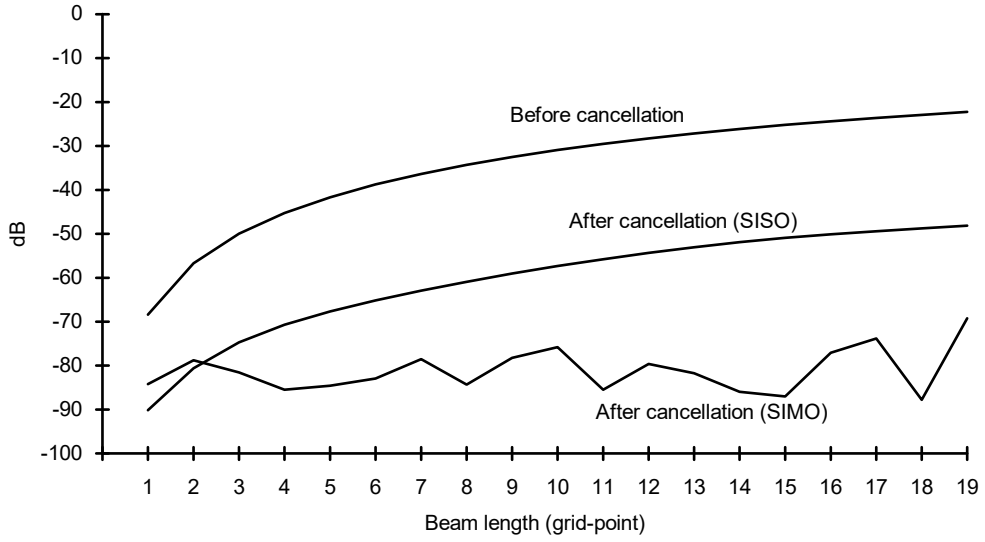

Figure 10. Average auto-power spectral density of the disturbance along the fixed-free beam before and after cancellation with the SISO and SIMO self-tuning AVC systems.

4. Conclusion

An approach for the design and implementation of a self-tuning active control system for noise cancellation and vibration suppression has been presented. Active control for noise cancellation and vibration suppression utilises the superposition of waves by artificially generating cancelling source(s) to destructively interfere with the unwanted source and thus result in cancellation. An active control mechanism for broadband cancellation of noise and vibration has been developed within an adaptive control framework. The algorithm thus developed and implemented incorporates on-line design and implementation of the controller in real-time. Moreover, a supervisory level control has been incorporated within the control mechanism allowing on-line monitoring of system performance and controller adaptation. The performance of the algorithm has been verified in the cancellation of broadband noise in a free-field medium

and in the suppression of broadband vibration in a flexible beam system. A significant amount of cancellation has been achieved over the full frequency range of the disturbance in each case. It has been noted that the level of cancellation achieved increases with an active control system incorporating a multiple set of cancelling sources. However, for the performance of the system to be robust, the design involving additional sources is to include suitable geometrical compositions of system components.

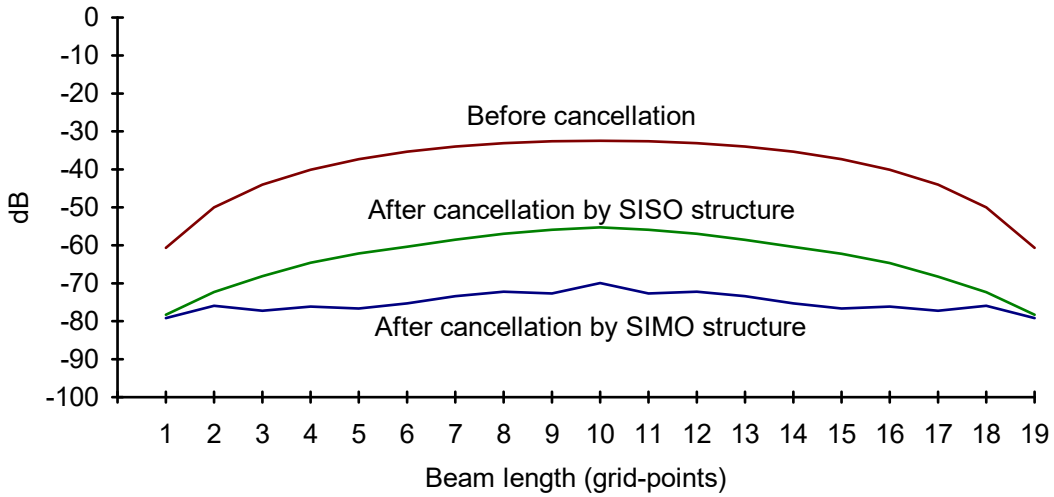

Figure 11. Average auto-power spectral densities of the disturbance along the fixed-fixed beam before and after cancellation with the SISO and SIMO self-tuning AVC system.

5. References

[1] R. R. Leitch and M. O. Tokhi: Active noise control systems. *IEE Proceedings-A*, **134** (1987), 525-546.

[2] P. Lueg: Process of silencing sound oscillations, US Patent 2 043 416, 1936.

[3] D. Guicking: Active noise control - A review based on patent specifications. In *Proceedings of Noise-93: International Conference on Noise and Vibration Control*, St Petersburg, **2** (1993), 153-157.

[4] D. Guicking: An overview of ASVC: from laboratory curiosity to commercial products. In *M. O. Tokhi and S. M. Veres (eds): Active control of sound and vibration*, The Institution of Electrical Engineers, London, 2002, 3–24.

[5] H. G. Leventhall: Active attenuators - A historical review and some recent developments, In *Proceedings of Inter-noise 80: International Conference on Noise Control Engineering*, Florida, **II** (1980), 679-682.

[6] G. E. Warnaka: Active attenuation of noise: the state of the art. *Noise Control Engineering*, **18** (1982), 100-110.

[7] M. O. Tokhi, and R. R. Leitch: Design of active noise control systems operating in three-dimensional non-dispersive propagation medium. *Noise Control Engineering Journal*, **36** (1991), 41-53.

[8] W. B. Conover: Fighting noise with noise. *Noise Control*, **2** (1956), 78-82 & 92.

[9] J. C. Burgess: Active adaptive sound control in a duct: A computer simulation. *Journal of the Acoustical Society of America*, **70** (1981), 715-726.

[10] B.Chaplin: The cancellation of repetitive noise and vibration. In *Proceedings of Inter-noise 80: International Conference on Noise Control Engineering*, Florida, **II** (1980), 699-702.
[11] S. J. Elliott and P. A. Nelson: An adaptive algorithm for multichannel active control, *Proceedings of the Institute of Acoustics*, **8** (1986), (Part 1), 135-147.
[12] S. J. Elliott, I. M. Stothers, and P. A. Nelson: A multiple error LMS algorithm and its application to the active control of sound and vibration. *IEEE Transactions on Acoustics, Speech, and Signal Processing*, **35** (1987), 1423-1434.
[13] C. F. Ross: An adaptive digital filter for broadband active sound control. *Journal of Sound and Vibration*, **80** (1982), 381-388.
[14] G. B. B. Chaplin, and R. A. Smith: Active control of repetitive noise and vibration. *Proceedings of the Institute of Acoustics*, February 1981, 9-12.
[15] G. B. B. Chaplin, R. A. Smith, and T. P. C. Bramer: Methods and apparatus for reducing repetitive noise entering the ear, US Patent No. 4 654 871, 1987.
[16] R. L. Clark, and C. R. Fuller: Control of sound radiation with adaptive structures. *Journal of Intelligent Systems and Structures*, **2** (1991), 431-452.
[17] P. J. Dines: Comparison of least squares estimation and impulse response techniques for active control of flame noise. *Proceedings of the Institute of Acoustics*, November 1982, F2.1-F2.4.
[18] L. J. Eriksson, M. C. Allie and R. A. Greiner: The selection and application of an IIR adaptive filter for use in active sound attenuation, *IEEE Transactions on Acoustics, Speech, and Signal Processing*, **35** (1987), 433-437.
[19] L. J. Eriksson, M. C. Allie, C. D. Bremigan and R. A. Greiner: Active noise control using adaptive digital signal processing. *Proceedings of IEEE International Conference on Acoustics, Speech, and Signal Processing*, **5** (1988), 2594-2597.
[20] C. R. Fuller, C. A. Rogers, and H. H. Robertshaw: Control of sound radiation with active/adaptive structures. *Journal of Sound and Vibration*, **157** (1992), 19-39.
[21] A. Roure: Self-adaptive broadband active sound control system. *Journal of Sound and Vibration*, **101** (1985), 429-441.
[22] A. Roure and B. Nayroles: Autoadaptive broadband active absorption in ducts by the means of transversal filtering. *Proceedings of Inter-noise 84: International Conference on Noise Control Engineering*, Honolulu, **I** (1984), 493-496.
[23] P. Sjösten: Experiences of an adaptive control system for active noise control. *Proceedings of Inter-noise 85: International conference on Noise Control Engineering*, Munich, **I** (1985), 595-598.
[24] S. D. Snyder and C. H. Hansen: Design considerations for active noise control systems implementing the multiple input, multiple output LMS algorithm. *Journal of Sound and Vibration*, **159** (1992), 157-174.
[25] M. O. Tokhi and R. R. Leitch: Self-tuning active noise control. *IEE Digest No. 1989/46: Colloquium on Adaptive Filtering*, London, 22 March 1989, 9/1-9/4.
[26] M. O. Tokhi and R. R. Leitch: Design and implementation of self-tuning active noise control systems. *IEE Proceedings-D: Control Theory and Applications*, **138** (1991), 421-430.
[27] M. O. Tokhi and S. M. Veres, (eds): Active control of sound and vibration. The Institution of Electrical Engineers, London, 2002.
[28] M. O. Tokhi and K. Mamour: Active control of noise in three-dimensional propagation. In *M. O. Tokhi and S. M. Veres (eds): Active control of sound and vibration*, The Institution of Electrical Engineers, London, 2002, 25–55.
[29] N. Hesselmann: Investigation of noise reduction on a 100 kVA transformer tank by means of active methods. *Applied Acoustics*, **11** (1978), 27-34.

[30] C. F. Ross: Experiments on the active control of transformer noise. *Journal of Sound and Vibration*, **61** (1978), 473-480.
[31] M. L. Munjal and L. J. Eriksson: An analytical, one-dimensional, standing-wave model of a linear active noise control system in a duct. *The Journal of the Acoustical Society of America*, **84** (1988), 1086-1093.
[32] A. J. Bullmore, P. A. Nelson, A. R. D. Curtis and S. J. Elliott: The active minimization of harmonic enclosed sound fields, Part II: A computer simulation. *Journal of Sound and Vibration*, **117** (1987), 15-33.
[33] S. J. Elliott, A. R. D. Curtis, A. J. Bullmore and P. A. Nelson: The active minimization of harmonic enclosed sound fields, Part III: Experimental verification. *Journal of Sound and Vibration*, **117** (1987), 35-58.
[34] P. A. Nelson, A. R. D. Curtis, S. J. Elliott and A. J. Bullmore: The active minimization of harmonic enclosed sound fields, Part I: Theory. *Journal of Sound and Vibration*, **117** (1987), 1-13.
[35] R. R. Leitch, and M. O. Tokhi: The implementation of active noise control systems using digital signal processing techniques. *Proceedings of The Institute of Acoustics*, **8**, (Part 1), (1986), 149-157.
[36] M. O. Tokhi and R. R. Leitch: The robust design of active noise control systems based on relative stability measures. *The Journal of the Acoustical Society of America*, **90** (1991), 334-345.
[37] M. O. Tokhi: Analysis and robust design of active noise control systems incorporating compact sources. *International Journal of Active Control*, **1** (1995), 109-144.
[38] C. J. Harris and S. A. Billings, (eds): Self-tuning and adaptive control: Theory and applications. Peter Peregrinus, London, 1981.
[39] M. O. Tokhi and R. R. Leitch: Active noise control. Clarendon Press, Oxford, 1992.
[40] P. E. Wellstead and M. B. Zarrop: Self-tuning systems - Control and signal processing. John Wiley, Chichester, 1991.
[41] G. S. Virk and P. K. Kourmoulis: On the simulation of systems governed partial differential equations. *Proceedings of IEE Conference on Control-88*, (1988), 318-321.
[42] M. A. Hossain and M. O. Tokhi: Evolutionary adaptive active vibration control. *Proceeding Institution of Mechanical Engineers*, **21** (1997), 183-193.
[43] M. A. Hossain: Digital signal processing and parallel processing for real-time adaptive noise and vibration control. *PhD Theses*, Department of Automatic Control and Systems Engineering, The University of Sheffield, UK, 1995.